Accepted Manuscript

Recognition and characterisation of high-grade ignimbrites from the neoproterozoic rhyolitic volcanism in southernmost Brazil

Carlos Augusto Sommer, Evandro Fernandes de Lima, Adriane Machado, Lucas Magalhães May Rossetti, Ronaldo Pierosan

PII: S0895-9811(13)00098-9

DOI: 10.1016/j.jsames.2013.07.010

Reference: SAMES 1197

To appear in: *Journal of South American Earth Sciences*

Received Date: 15 November 2012

Accepted Date: 22 July 2013

Please cite this article as: Sommer, C.A., Fernandes de Lima, E., Machado, A., May Rossetti, L.M., Pierosan, R., Recognition and characterisation of high-grade ignimbrites from the neoproterozoic rhyolitic volcanism in southernmost Brazil, *Journal of South American Earth Sciences* (2013), doi: 10.1016/j.jsames.2013.07.010.

- High-grade ignimbrites occur in a Neoproterozoic sequence in Southernmost Brazil.
- They are associated to a high-silica Na-alkaline magmatism.
- Rheomorphic deposits occur in the upper portion of the pyroclastic sequence.
- The pre-eruptive temperature obtained shows values between 850-978^{o}C .
- The high grade of the welding and the rheomorphism are sin-depositional process.

RECOGNITION AND CHARACTERISATION OF HIGH-GRADE IGNIMBRITES FROM THE NEOPROTEROZOIC RHYOLITIC VOLCANISM IN SOUTHERNMOST BRAZIL

Carlos Augusto Sommer[a*], Evandro Fernandes de Lima[a], Adriane Machado[b], Lucas Magalhães May Rossetti[a], Ronaldo Pierosan[c]

[a]Instituto de Geociências, Universidade Federal do Rio Grande do Sul, Av. Bento Gonçalves, 9500, Prédio 43136, Caixa Postal: 15001, Agronomia, CEP: 91501-970 / Porto Alegre, RS, Brasil. e-mails: evandro.lima@ufrgs.br; *** Corresponding author**: casommer@sinos.net; Phone: 55-51-33087398; FAX: 55-51-33087302.

[b]Centro de Geofísica da Universidade de Coimbra-CGUC, Av. Dr. Dias da Silva, 3000-134, Coimbra, Portugal. e-mail: adrianemachado@ci.uc.pt

[c] Instituto de Geociências, Universidade Federal do Mato Grosso, Av. Fernando Corrêa da Costa, nº 2367 - Bairro Boa Esperança. Cuiabá - MT - CEP: 78060-900. *e-mail: ronaldo.pierosan@hotmail.com*

Abstract - Neoproterozoic magmatism in southern Brazil is associated with translithospheric shear belts and strike-slip basins in a post-collisional setting related to the last stages of the Brasilian-Pan African Orogenic Cycle. It evolved from an association of high-K calc-alkaline, leucocratic-peraluminous and continental tholeiitic magmas, to an association with shoshonitic magmas and, eventually, to an association with magmas of the sodic mildly alkaline series. This magmatism varies from metaluminous to peralkaline and exhibits alkaline sodic affinity. A large volcanism is related to this alkaline sodic magmatism and is named the Acampamento Velho Formation. This unit was coeval with subaerial siliciclastic sedimentation in post-collisional basins preserved in the region. The Acampamento Velho Formation consists of pyroclastic and effusive volcanic deposits, which are mainly silicic, emplaced under subaerial conditions. The best exposures of this volcanism occur on the Ramada and Taquarembó plateaus, located southwest of Rio Grande do Sul in southernmost Brazil. The pyroclastic flow deposits are composed mainly of juvenile fragments such as pumices, shards and crystal fragments. Welding is very effective in these units. High-grade ignimbrites occur at the base and intermediate portions of the deposits and rheoignimbrites are observed at the top. The pre-eruptive temperature calculations, which were obtained at the saturation of zircon, revealed values between 870^{o}C–978^{o}C for Taquarembó Plateau and 850^{o}C–946^{o}C for Ramada Plateau. The calculated viscosity values vary from 6.946 to 8.453 logη (Pas) for the rheoignimbrites and 7.818 to 10.588 logη (Pas) for the ignimbrites. Zr contents increase toward the top of the pyroclastic sequence, which indicates an increase in peralkalinity and determines the reduction in viscosity for clasts at the upper portions of the flows. The patterns of the structures of the ignimbrites and rheoignimbrites in the Taquarembó and Ramada plateaus accords well with successive pyroclastic flows that halts en masse. In this model the entire pyroclastic flow halts en masse, so complex vertical changes in grain size and composition are interpreted as recording deposition from successive discrete

pyroclastic flows. The stratification observed in intermediate units in Taquarembó Plateau might reflect in this case variation in eruptive dynamics and short pauses.

Keywords: welding; rheomorphism; ignimbrites; high-silica; Neoproterozoic.

1. Introduction

Welding in eruptive volcanic products is an efficient deformation mechanism that involves the simultaneous sintering of vesicular and partially melted fragments in high-temperature flow deposits (Smith, 1960b; Guest and Rogers, 1967; Riehle et al., 1995). Welding results in definite textural and physical features (occurrence of fiamme, eutaxitic or parataxitic fabric, low porosity, deformation or pyroclastic particles) which are sometimes observed in ignimbrites (Smith, 1960a, 1960b, 1979; Ross and Smith, 1961; Ragan and Sheridan, 1972; Peterson, 1979; Streck and Grunder, 1995; Quane and Russell, 2005). Several authors involving theoretical and experimental aspects have considered that welding may be influenced by interactions between the eruption, flow dynamics and cooling of volcanic deposits. The welding process can be extreme for high-grade pyroclastic flow deposits (Walker 1983), where certain portions, called lava-like ignimbrites, are texturally indistinguishable from lava flows (Ekren et al., 1984; Henry et al., 1988). During and/or after deposition, the structures are formed by deformation caused by non-particulate flows, which is a continuous process known as rheomorphism (Schmincke and Swanson, 1967; Chapin and Lowell, 1979; Wolff and Wright, 1981; Branney et al., 1992).

High-grade ignimbrites occur in many volcanic settings and are sustained by alkali-rich magmas and encompass a wide compositional spectrum, which varies from basalts to rhyolites (Chapin and Lowell, 1979; Branney et al., 1992; Freundt, 1998). However, the most documented examples, which are from systems with high magmatic temperatures and elevated amounts of viscosity-reducing elements, have a peralkaline rhyolitic composition and

also low lithic content (Schmincke and Swanson, 1967; Schmincke, 1974; Wolff and Wright, 1981; Mahood, 1984; Kobberger and Schmincke, 1999).

In Brazil, welded deposits were spotted in several ancient volcanic sequences, from Paleoproterozoic to Neoproterozoic volcanic settings. They are normally associated with silicic volcanism, where high-grade and rheomorphic ignimbrites are common (Sommer et al., 1999, 2003, 2005, 2006; Barros et al., 2001; Pierosan et al., 2011; Barreto et al., 2013).

In this work, we discuss the welding significance of the rhyolitic ignimbrites of the Neoproterozoic Acampamento Velho Formation in southernmost Brazil. We also combine and integrate detailed fieldwork descriptions of this unit with petrography and lithochemistry. The terminology adopted to the characterization of the ignimbrite lithofacies is similar to Branney and Kokelaar (2002), combining grain size, depositional structures and fabric. The facies association was defined on the basis of volcanic units as pyroclastic flow (Table 1).

The Acampamento Velho Formation is characterised by a non-deformed and non-metamorphosed silicic volcanic succession situated in the western portion of the Sul-Rio-Grandense Shield. The un-altered preservation of the volcanics and previous detailed characterisation of the deposits and their regional context (e.g. Ribeiro et al., 1966; Wildner et al., 1999, 2002; Sommer et al., 1999, 2003, 2005, 2006; Almeida et al., 2002), has facilitated this further detailed investigation of the emplacement and welding characteristics of the ignimbrites in the Acampamento Velho Formation.

TABLE 1

2. Analytical procedures

The lithochemical studies are based on chemical analyses of ignimbrites that represent different lithotypes. The major and trace elements were analysed at Activation Laboratories Ltd., in Ontario, Canada, by using the ICP technique (Inductively Coupled Plasma) for major

elements and ICP-MS (Inductively Coupled Plasma Microspectrometry) for trace and rare earth elements.

Temperature data were calculated using Watson (1979) and Watson and Harrison (1983) methodologies that involve whole-rock chemical composition (major elements and Zr), which were applied to compositions of H2O > 2% and M parameter values between 0.9 and 2.1 [M = (Na+K+2×Ca)/(Al×Si) (Hanchar and Watson, 2003). Other temperature data were obtained by the Sisson and Grove (1993) methodology, which involves only compositions of the major elements.

Viscosity data were calculated using the model of the Giordano et al. (2008). This model predicts the non-Arrhenian Newtonian viscosity of silicate melts as a function of T and melt composition, including the volatile constituents (H2O and F). This model was based on experimental measurements of viscosity at T(K) on melts of known composition at atmospheric pressure (10^5 Pa). It is continuous in composition- and temperature-space and predicts the viscosity of natural volatile-bearing silicate melts (SiO_2, Al_2O_3, TiO_2, FeO_{tot}, CaO, MgO, MnO, Na_2O, K_2O, P_2O_5, H_2O, F_2O^{-1}) over fifteen log units of viscosity (10^{-1}–10^{14} Pa s). This model is capable of accommodating strong and fragile behavior of silicate melts (respectively, near- and non-Arrhenian T-dependences) and it reproduces observed relationships between melt composition and transport properties (i.e. glass transition temperature and fragility).

3. Geological setting

The Neoproterozoic lithologic section in southernmost Brazil is characterised mainly by plutonism along major translithopheric shear belts and by plutonism, volcanism and sedimentation in strike-slip basins such as the Camaquã. This volcano-sedimentary section is situated in relatively non-deformed areas and positioned on a basement of older igneous and metamorphic terrains (Fig. 1). The basin was formed during the post-collisional stages

(Liégeois, 1998) of the Brasiliano-Pan-African orogeny and is considered a strike-slip basin, although controversies exist regarding its classification and mechanism of generation (Almeida et al., 1981; Brito Neves and Cordani, 1991; Fernandes et al., 1992; Chemale, Jr., 2000; Paim et al., 2000). In this work, the post-collisional stage was considered as tectonically complex period, subsequent to the main collision stage that includes great movements along the shear zones, oblique collision, lithospheric delamination, rifting, subduction of small oceanic plates and volcanism associated with the basin sedimentation (Liégeois, 1998; Bonin, 2004).

Regarding the geological evolution, the basin can be interpreted as a depositional locus characterised by alternating depositional events and erosive intervals. The depositional episodes were dominated by the accumulation of sedimentary and volcano-sedimentary sequences with kilometric thickness. In the filling phases, the volcanic units are predominant at the base of the units followed by the predominant deposition of siliciclastic sediments. This dynamic context, which involved igneous, sedimentary and deformational events, generated a complex filling pattern represented by a series of stratigraphic units (Paim et al., 2000).

The Neoproterozoic-Ordovician magmatism of the Camaquã Basin evolved from tholeiitic and high K calc-alkaline magmas to shoshonitic and sodic alkaline magmas. The crustal contribution is represented by peraluminous granitoids (Wildner et al., 2002; Sommer et al., 2006; Lima et al., 2007) (Fig. 1).

The older volcanic rocks have compositions that are predominantly intermediate with shoshonitic affinity, with minor basic and acid compositions (Hilário Formation—Ribeiro and Fantinel, 1978 or Hilário Alloformation—Paim et al., 2000). U-Pb and Ar-Ar data obtained from volcanic rocks of the Hilário Formation suggest ages from 585 Ma to 590 Ma (Janikian et al., 2008).

The sodic-alkaline volcanism, named the Acampamento Velho Formation (Ribeiro and Fantinel, 1978) or Acampamento Velho Alloformation (Paim et al., 2000), succeeded the

shoshonitic magmatism and was formed of predominantly silicic explosive/effusive deposits. U-Pb SHRIMP analyses of zircon crystals extracted from rhyolites of the Passo do Salsinho area identified their ages *ca.*574 Ma (Chemale Jr., 2000; Janikian et al., 2008) and *ca.* 550 Ma for rhyolites from the Ramada Plateau area (Sommer et al., 2005).

The last volcanic manifestations of the Camaquã Basin (RodeioVelho Member, Ribeiro and Fantinel, 1978 or RodeioVelho Andesite, Paim et al., 2000) are represented by basalts with moderately alkaline-tholeiitic affinity and andesites with ages *ca.* 535 Ma (Almeida et al., 2010).

FIGURE 1

4. Acampamento Velho Formation—volcanic evolution and stratigraphic framework

This unit is characterised by rocks with basic-silicic composition and represented by the erupted portion of a voluminous sodic, silica-saturated, alkaline magmatism, which is mostly metaluminous with minor peralkaline components (Nardi and Bonin 1991; Sommer et al., 2005, 2006). The volcanic activity occurred under subaerial conditions and is exposed mainly in volcanic plateaus and ridges that are composed mostly of silicic lavas and pyroclastic deposits with minor intermediate and basic components (Wildner et al., 2002; Almeida et al., 2002; Sommer et al., 2005). Eruptive periods generally initiated with explosive episodes and closed with effusive events, which suggests a decrease in volatile activity throughout the progress of volcanic eruption and represents a complete volcanic eruptive cycle.

An important characteristic of the Acampamento Velho Formation is the predominance of sub-horizontal ignimbrites (about 80% of the total volcanic sequence) that

178 formed plateaus with areas around 300-400km^2, with an average thickness of 100m. These
179 deposits still preserve typical features from primary pyroclastic processes. Their features are
180 indicative of high-temperature flows with gases exsolved in the liquid during the
181 fragmentation. These attributes may suggest a subaerial volcanism most likely related to
182 caldera formation. The main units are pyroclastic flow deposits that are comprised primarily
183 of ignimbrites generally covered by rhyolitic lavas.

184 The stratigraphic organisation of the Acampamento Velho Formation was suggested
185 by Wildner et al. (1999), Almeida et al. (2002) and Sommer et al. (1999, 2005), who
186 considered that the best exposures of this unit are localised in Vila Nova do Sul (Ramada
187 Plateau) and Dom Pedrito (Taquarembó Plateau) (Fig. 2).

188

189

190 **FIGURE 2**

191

192 The silicic rocks from the Acampamento Velho volcanism generally reveal SiO_2
193 contents above 70 wt% and FeOt/(FeOt+MgO) ratios greater than 0.9, which is typical of
194 alkaline rhyolites (Ewart, 1979) (Fig. 3). They present a predominant metaluminous character
195 to comenditic peralkaline character (MacDonald, 1974; Le Maitre, 2002), although
196 subalkaline rocks are also observed (Wildner et al., 1999; Sommer et al., 2005; Sommer et al.,
197 2006; Lima et al., 2007). The predominant peralkaline character in silicic rocks is suggested
198 by the high Zr content (Leat et al., 1986). The trace elements from rhyolites exhibit patterns
199 similar to the granitic rocks of an intra-plate environment. The high Ce/Nb ratio is similar to
200 the post-orogenic magmatic associations (Leat et al., 1986). REE patterns are typical of
201 alkaline series with LREE enrichment relative to HREE. (Fig. 3)

202 Several authors have suggested a mantle source for the Acampamento Velho

magmatism. The Rb, Sr, Sm and Nd isotopic data combined with the trace elements in geochemistry suggest an EMI source for the rock type in the Taquarembó Plateau (Gastal and Lafon, 1998; Wildner et al., 1999; Chemale et al., 1999).

FIGURE 3

4.1. Geology of the Taquarembó Plateau

The Taquarembó plateau has an average thickness of 150m, and is composed of two stratigraphic units (Sommer et al., 1999). The older one is a succession of shoshonitic basic-intermediate lava-flows and volcanogenic sedimentary deposits from Hilario Formation. The younger unit is constituted of silicic lava flows separated by pyroclastic deposits (Acampamento Velho Formation) (Figs. 2 and 4). The basement units are composed of Paleoproterozoic granulite terranes and Neoproterozoic sedimentary sequences.

The silicic volcanism can be divided into 3 subaerial main eruptive cycles that reflect variations in the volcanic activity of this sequence (Fig. 2 and 4). The first cycle is characterised by trachytic-rhyolitic lava flows. The second cycle is characterised by explosive volcanic activity, which was responsible for the formation of ignimbritic deposits. The last cycle was formed of lava flows with compositions similar to the first cycle. After the release of volatiles and subsequent pyroclastic activity, the explosive activity prompted new effusive events that produced effusive rocks with compositions similar to effusive cycle one.

4.1.1. Ignimbrites facies

The ignimbrites were deposited in areas with horizontal topography without effective gravity control of rheomorphic movements. Three cooling units with thicknesses lower than 30 m were identified in ignimbritic deposits from the Taquarembó Plateau and most likely

correspond to three pyroclastic flow events, named flow 1, flow 2 and flow 3.

The first cooling unit is poorly sorted, massive, relatively homogeneous and has a higher concentration of lithic fragments at the lower portion (mL(nl)), which are predominantly lapilli-sized and from andesite (accidental) and rhyolites lavas (cognate).The top (eLT) is rich in pumices and strongly flattened shards (eutaxitic and parataxitic textures) and exhibits a high degree of welding with features indicative of rheomorphism (Fig 4 and 5).

The intermediate cooling unit corresponds to flow 2 where the ignimbrites are organised in successive sub-horizontal layers. The basal level of this unit is approximately 1 m thick and reveals a micro-cross lamination, which is mainly composed of shards and pumices with fine (< 1 mm) grainsize labeled xsT and can represent a ground surge level (Sommer et al., 1999). The origin of the stratification can be related to the different depositional unit successions, which were deposited almost simultaneously, working as one cooling unit (Fig. 4). The stratification is marked by the intercalation of layers that contain different proportions of the lithics-pumice composition. In general, they are laterally continuous (hundreds of meters) and 1 m thick and display smooth normal grading with lithic lapilli fragments and reverse grading in pumices sL(nlip), as evidenced by the greater amount of fiamme toward the top of the layers. The deposits consist predominantly of lapilli- and ash-sized pyroclasts, are represented by lithic fragments (ignimbrites and rare andesitic rocks), crystal fragments (alkali feldspar and quartz, pumices and other glass shards). An eutaxitic texture is the main structural feature and occurs in portions of the deposit where the welding is more intense. Axiolitic and spherulitic textures are common devitrification features. Adhesion and deformation of pumice and shards with a cusped habit occur at the matrix (Fig. 5). Some pumices maintain their original morphology, which may be related to the high concentration of lithic, rigid fragments which had limited plastic deformation. In the middle portion of the unit 2 occur a level rich in ignimbrites and obsidian fragments with size since 6.5 to 20 cm (sLB).

The rheomorphic ignimbrites, which occur at the upper portion of the pyroclastic flow sequence (unit 3), exhibit approximate thicknesses of 14 m and their contact is marked by erosive discordance. These ignimbrites are different from the ignimbrites on the underlying level, because they are homogeneous, porphyritic and exhibit an aphanitic vitriclastic matrix (Figs. 4 and 5). The deposits are massive, poorly sorted and show a slight enrichment in lapilli ignimbrites fragments on the bottom (2-4 mm), whereas an enrichment of crystals is observed toward the top (rheomLT). A strong flattening of glass shards and pumices is often observed, as well as parataxitic texture that involves quartz and K-feldspar crystals. Rotational structures in crystal fragments are common and associated with features of higher stretching. Spherulitic and axiolitic textures are also observed (Fig. 5).

FIGURE 4

FIGURE5

4.2. Geology of the Ramada Plateau

The Ramada Plateau (Fig. 1) covers an area of 24 km (E–W) by 12 km (N–S) and is about 120 m high. It is comprised mainly of subaerial volcanic succession characterized by silicic pyroclastic flow deposits, mafic to acidic lava flows, besides of shallow intrusions (Fig. 2). The basement units are composed of gneisses and tonalite associations with juvenile isotopic signature and Neoproterozoic sedimentary sequences. The lower portion of the Ramada Plateau is comprised of andesitic lava flow deposits, followed by volcanogenic conglomerates observed mainly in the eastern part of the plateau (Hilário Formation). This unit is overlain by basic-silicic volcanism (Acampamento Velho Formation) and characterised by the following (Fig. 2): (1) silicic ignimbritic deposits in near-horizontal layers (60–80 m

thick); (2) basic dykes (1–3 m thick) that cut the pyroclastic sequence; (3) rhyolitic lava flows (20–30 m thick) that overlie the pyroclastic deposits with complex flow foliation and most likely erupted along fractures; and (4) mafic lava flows intercalated with the upper silicic lava flow sequence and restricted to a small portion northwest of the plateau. Subvolcanic silicic intrusions cut the andesitic basal unit and country rocks around the Ramada Plateau. Dykes and sills (1–5 m thick) are the dominant intrusions, although domes with NW–SE and NE–SW orientations are observed. These subvolcanic intrusions represent probably feeder dykes and lie below a complex system of ancient vents for volcanism of the Ramada Plateau.

4.2.1. Ignimbrites facies

All ignimbritic exposures, which were deposited on areas with horizontal topography, indicate a higher degree of welding and an approximate thickness of 60 m. The ignimbritic facies association, which suggests a formation from 3 distinct cooling units, produced deposits that display similar characteristics. The ignimbrites from unit 1 are roughly 20 m thick and exhibit a tabular geometry. They are massive, poorly sorted and abundant in lapilli-sized subangular lithic fragments (mLT). Rhyolitic cognate fragments are prevalent, but accidental lithic fragments are observed too (granitoids, andesites and sandstones fragments). The matrix is ash-sized and composed mainly of glass shards and pumices lapilli. Crystal fragments of quartz and K-feldspar also compose the matrix (Fig. 6).

The deposits of the unit 2 are 25 m thick on average and occur disposed in tabular geometry. This unit is poorly sorted and shows lateral gradational changes in ignimbrites with abundant lithic fragments and pumice lapillis. K-feldspar and quartz phenocrystal fragments are also present. Ignimbrites are separated into two main facies: lenticulites and crystal-rich deposits. The lenticulite facies consist of a welded rhyolitic ignimbrite with vitriclastic matrix and alkaline feldspar, quartz, pumice fragments and rare lithic lappili (//bpL). In general pumices are flattened and aligned, defining a planar foliation subparallel to bedding. The

lenticular aspect and eutaxitic texture are a result of high-grade welding of the deposit. The matrix generally involves the quartz and K-feldspar crystals fragments with corrosion gulfs (Fig. 7). Axiolites and spherulites, which are common features of high-temperature devitrification processes, are observed mainly in the pumice fragments. Thin layers (0.4–0.6 m) of crystal-rich ignimbrite (crLT) overlie the lenticulites (Sommer et al., 2001). They have high crystal contents (50–60%) and are composed of K-feldspar (0.5–2.5 mm) and quartz (1–2 mm) phenocrystal. Rare pumice, accidental and cognate lithic fragments occur in an ash-sized matrix composed mainly of shards. Welding of the deposit generates an incipient eutaxitic texture. The high concentration of crystals in ignimbrites may be related to eruptions of highly crystallised magmas or physical fractionation during the flow (Cas and Wright, 1987).

The unit 3 of the ignimbrite sequence is characterised by rheomorphic ignimbrites (rheomT) with thicknesses of approximately 15 m that occur with tabular geometry. They are massive, aphanitic to porphyritic, with a vitriclastic matrix and ash-sized pyroclasts. A strong foliation is marked by the stretching of pumices and glass shards. The petrographic descriptions illustrate that contact among the constituents was obliterated and the external limit of the fragments disappeared. The foliation of the parataxitic texture involves alkaline feldspar and quartz that show rotational structures. Fiamme with a higher degree of stretching, transformed into spherulites and axiolites is common (Fig. 7).

FIGURE 6

FIGURE 7

5. Composition, temperature and viscosity data

Crystallisation and viscosity temperatures were estimated from the chemical

compositions of the rocks. They are necessary to discuss the welding mechanisms. For the Acampamento Velho Formation, the determination of these parameters was based on the chemical compositions of the ignimbrites and rheoignimbrites from the Taquarembó and Ramada plateaus (Table 2).

The ignimbrites of both sequences may be considered high-silica rocks because they generally have SiO_2 values that vary from 72 to 77 wt% (Table 2). They most likely crystallised from peralkaline liquids and due to a loss of alkali elements, exhibit maximum agpaitic index values near 1. The loss of these elements usually occurs during crystallisation, or is due to post-magmatic alteration processes (Leat et al., 1986). The original peralkaline affinity of this association is supported by high Zr contents, generally over 300 ppm (Leat et al., 1986). Zr contents are similar for the ignimbrites of the Taquarembó and Ramada plateaus and the highest values are found in the rheomorphic ignimbrites that were disposed in the upper sequence.

5.1. Temperature

The temperature data were estimated from the major elements and Zr contents, according to the method suggested by Watson (1979) and Watson and Harrison (1983). Furthermore, the *liquidus* temperature was calculated by following the Sisson and Grove (1993) systematics.

The zircon saturation data of the ignimbrites from the Taquarembó and Ramada plateaus indicate a temperature interval between 870°C and 978°C (Tab. 2). It is similar to the interval obtained for the *liquidus* temperature (903°C–953°C). These values are slightly higher than values registered by Streck and Grunder (1997) for the Rattlesnake Tuff Rhyolite, which displayed metaluminous affinity to slightly peralkaline affinity. Values of 850±50°C for the crystallisation temperature of zircon were obtained by Pierosan et al. (2011) for metaluminous acid ignimbrites from the Iricoumé Group. These results are similar to the results obtained for

representative rhyolites and granites of A-type magmatism (Clemens et al., 1986; King et al., 1997; Dall'Agnol et al., 1999; Hergt et al., 2007). Experimental data acquired by Patiño Douce (1997) indicate approximate temperatures of 950°C for the generation of A-type magmas.

The comparison of the calculated temperatures (Table 2 and Fig. 8) indicates higher magmatic values for the ignimbrites of the Taquarembó Plateau (870-978^{o}C) than the values estimated for the Ramada Plateau (850-946^{o}C). At the upper ignimbritic units of both plateaus, high magmatic temperatures were obtained for rheoignimbrites (average = 945^{o}C) that are consistent with the higher Zr contents in these lithotypes.

The higher degree of welding in these deposits combined with partial rheomorphism in some sections indicates little loss of heat during the origin and emplacement of these flows, which is common in low-eruptive columns. These deposits are dominated by juvenile fragments such as pumices, shards and massive vitreous fragments. The degree of welding, as observed in the ignimbrites of the Acampamento Velho Formation, is indicative of variable temperatures. The vertical variations in clast size and fragment type are observed at the intermediate and base portions. These variations are associated with pronounced eutaxitic texture, which partially maintains the clastic aspect of the deposit. The rheoignimbrites with parataxitic and micropoikilitic textures are concentrated at the upper deposit portions. They are generated by intense deformation of pumice and vitreous fragments and are associated with devitrification in high temperatures.

5.2. Viscosity

The viscosity obtained for the rocks from the Acampamento Velho Formation was calculated from data of the major elements using Giordano et al. (2008) model and values are shown in the table 2. As an initial parameter, we assumed an anhydrous condition, whereas

382 the temperature data were estimated by the Zr saturation method (Watson, 1979; Watson and
383 Harrison, 1983; Hanchar and Watson, 2003).

384 The calculated viscosity values vary from 6.946 to 8.453 logη (Pa s) for the
385 rheoignimbrites and 7.818 to 10.588 logη (Pa s) for the ignimbrites (Fig. 8). The highest
386 values were obtained from rheoignimbrites in the upper stratigraphic units (Table 1). These
387 results are similar to the results obtained for the Rattlesnake Tuff and Campanian Ignimbrite
388 (Giordano et al., 2006; 2008), and the Paleoproterozoic rhyolites from the Iricoumé Group
389 (Pierosan et al., 2011).

390

391 **FIGURE 8**

392

393 **TABLE 2**

394

395 **6. Discussion**

396 The ignimbrite deposits of the Taquarembó and Ramada plateaus exhibit a high degree
397 of welding, which may be indicative of high temperatures. Over most of their outcrop the
398 ignimbrites rests on a flat, horizontal paleosurface and forms a plateau with uniform thickness
399 and structural characteristics. The large amount of pumices and the low occurrence of lithics
400 are compatible with high-grade ignimbrites (Marti el al., 1991). Diagenitic features
401 (alteration, dissolution and mechanical compaction) were not observed and therefore cannot
402 be used to explain the presence of fiamme and eutaxitic texture. The high temperatures
403 obtained are close to the values discussed by Gründer et al. (2005) for the Rattlesnake Tuff
404 Ignimbrite that displays similar chemical affinity. Higher temperatures are observed for the
405 rheoignimbrites with Agpaitic Index around the unit and consequently, present lower
406 viscosity. It may explain the rheomorphism observed in this facies.

Experimental data for rhyolitic systems under anhydrous conditions indicate minimum welding temperatures between 900°C and 1000°C (Gründer et al., 2005), which are higher than temperatures observed in natural systems. Variations in H_2O content can reduce the minimum welding temperature to 600°C for metaluminous siliceous systems (Quane and Russell, 2005). According to Dingwell and Webb (1990), this temperature represents the kinetic limit between a liquid (viscous system) and a solid (elastic behavior) in reaction to applied mechanical stress. In this situation, the particles are viscous and deformed above the glass transition allowing for welding. Below this temperature, welding is inhibited. The difference in temperature between viscous and elastic limits in peralkaline systems may reach 100º C (Llambias, 2003). Therefore, compositional aspects are important for the understanding of welding origin, considering transition temperature of the glass for each chemical system. The influence of compaction and H_2O content in the welding of ignimbrites, which is associated with temperature, was also evaluated in experimental form by Gründer et al. (2005). The load pressure exerted over the accumulation of pyroclasts during flow has been assumed as one of the main factors responsible for the compaction and expulsion of interstitial gases (Smith, 1960). H_2O is another important factor in decreasing viscosity of magmas and its presence promotes viscous deformation (Shaw, 1972). According to Dingwell et al. (1996), low H_2O contents are typical in rhyolitic glasses and H_2O contents ranging from 0.2% to 0.4% are sufficient for causing the super saturation and liberation of volatile in rhyolitic magmas during rising, which substantially reduces magma viscosity and consequently inhibits the rapid loss of this phase. Lithostatic load larger than 1 MPa (600º C, 0.2% H_2O), which corresponds to a deposit thicker than 40 m, would be necessary to generate a welded deposit (Dingwell et al., 1996). Significantly higher pressures (5 MPa) have experimentally generated textures with high degrees of welding under equivalent temperatures and H_2O contents.

The cooling unit thickness is smaller than 30 m at the Taquarembó Plateau and this is

typical for peralkaline ignimbrites (Schmincke, 1974). The presence of crystallised quartz in these cooling units is common according to Schmincke, 1974. The same characteristics are observed in the Ramada Plateau cooling units. Rheoignimbrites with parataxitic texture are concentrated in the upper portions of the Taquarembó and Ramada plateaus, which display stretched vesicles filled with microcrystalline material.

The diversity of high-grade pyroclastic deposits leads to different model proposals for the origin and emplacement of these high-temperature flows. According to Schmincke and Swanson (1967), pyroclastic textures with strong deformation are generated from a viscous laminar flow in movement, where the agglutination of hot pyroclastic particles is gradually flattened and deformed when flow mass decelerates. Another model was proposed by Chapin and Lowell (1979), which considered that the agglutination and deformation of pyroclastic particles occur during the initial emplacement of a dense flow. These processes progressively become more intense in the base and lateral boundary layers during the filling of a valley.

Wolff and Wright (1981) postulated that the welding and rheomorphism are established after the transportation and deposition of pyroclastic flow. In this model, as well as in the Schmincke and Swanson (1967) model, the halt of the pyroclastic flow is required. The complex vertical changes in grain size and composition could be interpreted as deposition of successive pyroclastic flows.

Branney and Kokelaar (1992, 1997, 2002) assumed that the deposition of thick high-grade ignimbrites may be generally related to the rapid and continuous pyroclastic aggradation. In this manner, the changes in composition and eruption constituents would be registered in the ignimbrite vertical zoning. According to these authors, the massive lapilli tuff deposits are generated by progressive aggradational processes in the basal layer, with high concentrations of pyroclasts versus volatile, which are independent of the particle contents and higher degree of fluid turbulence. The high degree of welding and rheomorphism considered in this model is not restricted to very dense flows placed in valleys. The vertical

459 changes in welding intensity indicate modifications in viscosity of the clasts (temperature,
460 composition and volatile content) from the base that is aggraded during the flow. The
461 deformation of the deposit may continue after the pyroclastic material is supplied. The model
462 of agglutination that occurs during the progressive aggradational process shows the advantage
463 of explaining some vertical changes in grain size, composition and welding intensity in the
464 same pyroclastic flow. An important effect resulting of this process is the increase of average
465 particle size within the flow and this enhances settling rates. Another main effect is the
466 formation of a non-particulate and rheomorphic lower part of the flow. It is fed by the main
467 particulate turbulent flow. This non-particulate part may move relatively independently of
468 main flow and has as peculiar characteristics the presence of the mass flow structures. The
469 progressive homogenization of the liquid particles, and partial to complete obliteration of the
470 primary clastic structure may generate lava-like facies.

471 The patterns of the structures of the ignimbrites and rheoignimbrites in the
472 Taquarembó and Ramada plateaus accords well with successive pyroclastic flows that halts en
473 masse. In this model the entire pyroclastic flow halts en masse, so complex vertical changes in
474 grain size and composition are interpreted as recording deposition from successive discrete
475 pyroclastic flows (Schmincke and Swanson, 1967; Wolf and Wright, 1981). The stratification
476 observed in the intermediate units of the Taquarembó Plateau reflects in this case variation in
477 eruptive dynamics and short pauses of the volcanic activity.

478 The vertical variations in grain size, constituent type, degree of welding and increase
479 in Zr contents occurs towards the top of the plateaus, (rheoignimbrites - units 3).

480

481 **7. Conclusions**

482 Neoproterozoic volcanic deposits from the Acampamento Velho Formation were
483 formed under subaerial conditions in the Sul-Rio-Grandense Shield, which is located in
484 southernmost Brazil. Evidence of this volcanism can be found in the southwest region of the

Rio Grande do Sul plateaus. They are composed of ignimbrites and silicic effusive rocks. The geochemical affinity of the magmatism is compatible with metaluminous to peralkaline sodic series and associated with post-collisional stages. The higher degree of welding in these deposits combined with partial rheomorphism in some sections indicates little loss of heat during the origin and emplacement of these flows, which is common in low-eruptive columns. These deposits are dominated by juvenile fragments such as pumices, shards and massive vitreous fragments. The pre-eruptive temperature data obtained reveal high values. The degree of welding, as observed in the ignimbrites of the Acampamento Velho Formation, is indicative of variable temperatures. The vertical variations in clast size and fragment type are observed at the intermediate and base portions. These variations are associated with pronounced eutaxitic texture, which partially maintains the clastic aspect of the deposit. The rheoignimbrites with parataxitic and micropoikilitic textures are concentrated at the upper deposit portions. They are generated by intense deformation of pumice and vitreous fragments and are associated with devitrification in high temperatures. Stretched vesicles filled with microcrystalline quartz may have been generated by lateral migration of volatiles between the flow surfaces. The geochemical data indicate that the Zr contents increase towards the top of the pyroclastic sequence. This variation in Zr content also suggests an increase in peralkalinity. It may contribute to the reduction in viscosity of the clasts. The H_2O contribution is not discarded as an additional factor in the reduction of the viscosity, as well as the higher concentration of pumices in the rheoignimbrites and the liberation of the volatiles during deformation (Legros et al., 2000).

The high degree of welding and rheomorphism in the ignimbritic deposits from the Taquarembó and Ramada plateaus may be explained by the en masse model (Schmincke and Swanson, 1967; Wolf and Wright, 1981) .

Acknowledgements: We especially acknowledge the research grants and financial support of

the CNPq (303584/2009-2, 473683/2007, 5470641/2008-8, 470203/2007-2, 302213/2012-0, 471402/2012-5, 303038/2009-8 and 4705052010-9), FAPERGS (100798) and PRONEX (10/0045-6). We also thank the laboratory support from the IGEO/UFRGS. We thank L. Pioli, R. A. Fuck and anonymous reviewers for their valuable comments and constructive reviews.

References

Almeida, F.F.M., Hasui, Y., Brito Neves, B.B., 1981. Brazilian structural provinces: An introduction: Earth Sci. Rev. 17, 1–29.

Almeida, R.P., Janikian, L., Fragoso-Cesar, A.R.S., Fambrini, G.L., 2010. The Ediacaran to Cambrian Rift System of Southeastern South America: Tectonic Implications. J. Geol. 118: 145–161.

Almeida, D.P.M., Zerfass, H., Basei, M.A., Petry, K., Gomes, C.H., 2002. The Acampamento Velho Formation, a Lower Cambrian Bimodal Volcanic Package: Geochemical Stratigraphic Studies from the Cerro do Bugio, Perau Serra de Santa Bárbara (Caçapava do Sul, Rio Grande do Sul, RS – Brazil). Gondwana. Res. 5 (3), 721-733.

Barreto, C.J.S., Lafon, J.M., Costa, L.T.R., Lima, E.F. 2013. Vulcanismo félsico paleoproterozoico do Grupo Iricoumé, Domínio Erepecuru-Trombetas, Província Amazônia Central: dados de campo, caracterização petrográfica e geocronologia Pb-Pb em zircão. Geologia USP. Série Científica. 13, 47-72.

Barros, M.A.S., Fetter, A., Chemale Jr., F., Lima, E.F., 2001. Caracterização petrográfica e dados geocronológicos preliminares de rochas vulcânicas da Formação Iriri, porção centro-sul do Cráton Amazônico-Aripuanã-MT. Rev. Bras. Geoc. 31(3), 37-42.

Bonin, B., 2004. Do coeval mafic and felsic magmas in post-collisional to within-plate regimes necessarily imply two contrasting, mantle and crustal, sources? A review. Lithos. 78, 1-24.

536 Branney, M.J., Kokelaar, P., 1992. A Reappraisal of ignimbrite emplacement: progressive
537 aggradation and changes from particulate to non-particulate flow during emplacement of
538 high-grade ignimbrite. Bull. Volcanol. 54, 504-520.

539 Branney, M.J., Kokelaar, B.P., 1997. Giant bed from a sustained catastrophic density current
540 flowing over topography: Acatlan ignimbrite, Mexico. Geology. 25, 115-118.

541 Branney, M.J., Kokelaar, B.P., 2002. Pyroclastic density currents and the sedimentation of
542 ignimbrites. Geol. Soc. London Mem. 27, 152 pp.

543 Branney, M.J., Kokelaar, B.P., McConnell, B.J., 1992. The Bad Step Tuff: a lava-like
544 rheomorphic ignimbrite in a calc-alkaline piecemeal caldera, English Lake District. Bull.
545 Volcanol. 53, 187-199.

546 Brito-Neves, B.B., Cordani, U.G., 1991. Tectonic evolution of South America during Late
547 Proterozoic. Precambrian Res. 53, 23-40.

548 Cas, R.A.F., Wright, J.V., 1987. Volcanic succession, modern and ancient: a geological approach
549 to processes, products and successions. London, Allen & Unwin, 528p.

550 Chapin, C.E., Lowell, G.R., 1979. Primary and secondary flow structures in ash-flow tuffs of the
551 Gribbles Run paleovalley, central Colorado. Spec. Pap. Geol. Soc. Am. 180, 137–154.

552 Chemale Jr., F., 2000. Evolução Geológica do Escudo Sul-Rio-Grandense. In: Holz, M., De
553 Ros, L.F. (Eds.), Geologia do Rio Grande do Sul. Porto Alegre, CIGO/UFRGS, pp. 13-52.

554 Chemale Jr., F., Wildner, W., Lima, E.F., Van Schmus, W.R., 1999. Isotopic studies of
555 Brasiliano retro-arc magmatism in Southern Brazil. Anais do 1º Simpósio sobre vulcanismo e
556 ambientes associados, Gramado, RS, Brasil, 1, 57.

557 Clemens, J.D., Holloway, J.R., White, A.J.R., 1986. Origin of an A-type granite: experimental
558 constraints. Am. Mineral. 71, 317-324.

559 Dall'Agnol, R., Scaillet, B., Pichavant, M., 1999. An experimental study of a Lower

560 Proterozoic A-type granite from the eastern Amazonian Craton, Brazil. J. Petrol. 40(11),
561 1673-1698.

562 De La Roche H., Leterrier J., Grandclaude P., 1980. A classifícation of volcanic and plutonic
563 rocks and associations. Chem. Geol. 29,183-210.

564 Dingwell, D.B., Webb, S.L., 1990. Relaxation in silicate melts. Eur. J. Mineral. 2, 427–449.

565 Dingwell, D.B., Romano, C., Hess, K.U., 1996. The effect of water on the viscosity of
566 haplogranite melt under P-T-X conditions relevant to silicic volcanism. Contrib. Mineral.
567 Petr. 124, 19–28.

568 Ekren, E.B., Mc Intyre, D.H., Bennett, E.H., 1984. High-temperature, large-volume, lava-like
569 ash-flow tuff without calderas in southwestern Idaho. Prof. Pap. U.S. Geol. Surv. 1272, 1–76.

570 Ewart, A., 1979. A review of the mineralogy and chemistry of Tertiary-Recent dacitic, latitic,
571 rhyolitic and related salic volcanic rocks. In: Baker, F. (Ed.), Trondhjemites, dacites and related
572 rocks. The Hague: Elsevier, pp. 113-121

573 Fernandes, L.A.D., Tommasi, A., Porcher, C.C., 1992. Deformation patterns in the southern
574 Brazilian branch of the Dom Feliciano Belt: A reappraisal. J.S. Am. Earth Sci. 5(1), 77–96.

575 Freundt, A., 1998. The formation of high-grade ignimbrites. I. Experiments on high- and low-
576 concentration transport systems containing sticky particles. Bull. Volcanol. 59, 414–435.

577 Gastal, M.C.P., Lafon, J.M., 1998. Gênese e evolução dos granitóides metaluminosos de
578 afinidade alcalina da porção oeste do escudo sul-rio-grandense: geoquímica e isótopos de Rb-
579 Sr e Pb-Pb. Rev. Bras. Geoc. 28, 11-28.

580 Giordano, D., Mangiacapra, A., Potuzak, M., Russel, J.K., Romano, C., Dingwell, D.B., Di
581 Muro, A., 2006. An expanded non-Arrhenian model for silicate melt viscosity: A treatment
582 for metaluminous, peraluminous and peralkaline liquids. Chem. Geol. 229, 42-56.

583 Giordano, D., Russel, J.K., Dingwell, D.B., 2008. Viscosity of magmatic liquids: A model.

584 Earth and Plan. Sci. Lett. 271, 123–134.

585 Grunder, A.L., Laporte, D., Druitt, T.H., 2005. Experimental and textural investigation of
586 welding: effects of compaction, sintering, and vapor-phase crystallization in the rhyolitic
587 Rattlesnake Tuff. J. Volcanol. Geoth. Res. 142, 89–104.

588 Guest, J.E., Rogers, P.S., 1967. The sintering of glass and its relationship to welding in
589 ignimbrites. P. Geol. Soc. London. 1641, 174–177.

590 Hanchar, J.M., Watson, E.B., 2003. Zircon saturation thermometry. In: Hanchar, J.M. and
591 Hoskin, P.W.O. (Eds) Zircon. Rev. Min. Geochem. 53, 89–112.

592 Henry, C.D., Price, J.G., Rubin, J.N., Parker, D.F., Wolff, J.A., Self, S., Franklin, R., Barker,
593 D.S., 1988. Widespread, lava-like silicic volcanic rocks of Trans-Pecos Texas. Geology. 16,
594 509-512.

595 Hergt, J., Woodhead, J., Schofield, A., 2007. A-type magmatism in the Western Lachlan Fold
596 Belt? A study of granites and rhyolites from the Grampians region, Western Victoria. Lithos.
597 97, 122-139.

598 Janikian, L., Almeida, R.P., Trindade, R.I.F., Fragoso-Cesar, A.R.S., D'Agrella-Filho, M.S.,
599 Dantas, E.L., Tohver, E., 2008. The continental record of Ediacaran volcano-sedimentary
600 successions in southern Brazil and their global implications. Terra Nova. 20, 259–266.

601 King, P.L., White, A.J.R., Chappell, B.W., Allen, C.M., 1997. Characterization and Origin of
602 Aluminous A-type Granites from the Lachlan Fold Belt, Southeastern Australia. J. Petrol.
603 38(3), 371-391.

604 Kobberger, G., Schmincke, H.U., 1999. Deposition of rheomorphic ignimbrite D (Mogan
605 Formation) Gran Canaria, Canary Islands, Spain. Bull. Volcanol. 60, 465–485.

606 Le Maitre, R.W., 2002. Igneous rocks: a classification and glossary of terms. In:
607 Recommendations of the International Union of Geological Sciences Subcommission on the

608 Systematic of Igneous Rocks. Cambridge: Cambridge University Press. pp. 252.

609 Leat, P.T., Jackson, S.E., Thorpe, R.S., Stillman, C.J., 1986. Geochemistry of bimodal basalt -
610 subalkaline/peralkaline rhyolite provinces within the Southern British Caledonides. J. Geol. Soc.
611 London. 143, 259-273.

612 Legros, F., Sparks, R.S.J., Tait, S.R., Yaney, Y., 2000. Discussion on dense welding caused by
613 volatile resorption. J. Geol. Soc. London. 157, 893-895.

614 Liégeois, J.P., 1998. Preface – Some words on post-collisional magmatism. Lithos. 45, 15-17.

615 Lima, E.F., Sommer C.A., Nardi, L.V.S., 2007. O vulcanismo neoproterozóico-ordoviciano
616 no Escudo Sul-Rio-Grandense: os ciclos vulcânicos da Bacia do Camaquã. In: Iannuzzi, R.,
617 Frantz, J.C. (Eds.), 50 Anos de Geologia. Instituto de Geociências. Contribuições. Porto
618 Alegre: Comunicação e Identidade. 1, 79-95

619 Llambías, E.J., 2003. Geología de los Cuerpos Ígneos. Asociación Geológica Argentina, Serie
620 B Didáctica y complementaria, 27, Buenos Aires. pp. 182.

621 MacDonald, R., 1974. Nomenclature and Petrochemistry of the Peralkaline Oversaturated
622 Extrusive Rocks. Bull. Volcanol. 38, 498-516.

623 Mahood, G.A., 1984. Pyroclastic rocks and calderas associated with strongly peralkaline
624 magmatism. J. Geophys. Res. 89, 8540–8552.

625 Marti, J., Diez-Gil, J.L., Ortiz, R., 1991. Conduction model for the thermal influence of lithic
626 clasts in mixtures of hot gases and ejecta. J. Geophys. Res., 96, B13: 21879-21885.

627 Nakamura, N., 1974. Determination of REE, Ba, Fe, Mg, Na and K in carbonaceous and
628 ordinary chondrites. Geoch.Cosmoch. Acta. 38, 57-775.

629 Nardi, L.V.S., Bonin B., 1991. Post-orogenic and non-orogenic alkaline granite associations: the
630 Saibro intrusive suite, southern Brazil - a case study. Chem. Geol. 92, 197-212.

631 Paim, P.S.G., Chemale Jr., F., Lopes, R.C., 2000. A Bacia do Camaquã. In: Holz M., De Ros

L.F (Eds.), Geologia do Rio Grande do Sul. Porto Alegre, CIGO/UFRGS. pp. 231-374.

Patiño-Douce, A.E., 1997. Generation of metaluminous A-type granites by low-pressure melting of calc-alkaline granitoids. Geology. 25(8),743-746.

Pearce, J.A., Harris, N.B.W., Tindle, A.G., 1984. Trace element discrimination diagrams for the tectonic interpretation of granitic rocks. Journal of Petrology. 25 (4), 956-983.

Peterson, D.W., 1979. Significance of flattening of pumice fragments in ash-flow tuffs. In: Chapin, C.E., Elston, W.E. (Eds.), Ash-Flow Tuffs and Associate Igneous Rocks. Spec. Pap. Geol. Soc. Am. 180, 195–204.

Pierosan, R., Lima, E.F., Nardi, L.V.S, Campos, C.P., Bastos Neto, A.C., Ferron, J.M.T.M., Prado, M., 2011. Paleoproterozoic (~1.88Ga) felsic volcanism of the Iricoumé Group in the Pitinga Mining District area, Amazonian Craton, Brazil: insights in ancient volcanic processes from field and petrologic data. An. Acad. Bras. de Cienc. 83, 921-937.

Quane, S.L., Russell, J.K., 2005. Welding: insights from high-temperature analogue experiments. J. Volcanol. Geoth. Res. 142, 67–87.

Ragan, D.H., Sheridan, M.F., 1972. Compaction of the bishop Tuff, California. Geol. Soc. Am. Bull. 83, 95–106.

Ribeiro, M., Fantinel, L.M., 1978. Associações petrotectônicas do Escudo Sul-rio-grandense: I Tabulação e distribuição das associações petrotectônicas do Rio Grande do Sul. Iheringia, Série Geológica. 5, 19-54.

Ribeiro, M., Bocchi, P.R., Figueiredo Filho, P.M., Tessari, R., 1966. Geologia da Quadrícula de Caçapava do Sul. Rio Grande do Sul. Bol. Div. Fom. Prod. Min. Bras., Rio de Janeiro. 127, 1-232.

Riehle, J.R., Miller, T.F., Bailey, R.A., 1995. Cooling, degassing and compaction of rhyolitic ash-flow tuffs: a computational model. Bull. Volcanol. 57, 319–336.

Ross, C.S., Smith, R.L., 1961. Ash-flow tuffs, their origin, geologic relations and identification. Prof. Pap. U.S. Geol. Surv. 366, pp. 81.

Schmincke, H.U., 1974. Volcanological aspects of peralkaline silicic welded ash-flow tuffs. Bull. Volcanol. 38, 594–636.

Schmincke, H.U., Swanson, D.A., 1967. Laminar viscous flowage structures in ash-flow tuffs from Gran Canaria, Canary Islands. J. Geol. 75, 641-664.

Shaw, H.R., 1972. Viscosities of magmatic silicate liquids: an empirical model of prediction. Am. J. Sci. 272, 438– 475.

Sisson, T.W., Grove, T.L., 1993. Experimental investigations of the role of H_2O in calc-alkaline differentiation and subduction zone magmatism. Contrib. Mineral. Petr. 113, 143 - 166

Smith, R.L., 1960. Ash flows. Geol. Soc. Am. Bull. 71, 795-842.

Smith, R.L., 1960 b. Zones and zonal variations in welded ash-flows. Prof. Pap. U.S. Geol. Surv. 354-F, 149-159.

Smith, R.L., 1979. Ash-flow magmatism. In: Chapin, C.E., Elston, W.E. (Eds.), Ash-Flow Tuffs. Spec. Pap. Geol. Soc. Am. 180, 5–27.

Sommer, C.A., Lima, E.F., Nardi, L.V.S., 1999. Evolução do vulcanismo alcalino na porção sul do Platô do Taquarembó, Dom Pedrito – RS. Rev. Bras. Geoc. 29 (2), 245-254.

Sommer, C.A., Lima, E.F., Nardi, L.V.S., Liz, J.D., Matos, D., 2001. Ignimbritos ricos em cristais do Platô da Ramada - RS, Brasil. In: XI CONGRESSO LATINOAMERICANO DE GEOLOGIA, Montevideo, Uruguai, Actas... Base CD-Rom.

Sommer, C.A., Lima, E.F., Nardi, L.V.S., Liz, J.D., Pierosan, R., 2003. Depósitos de fluxo piroclástico primários: caracterização e estudo de um caso no vulcanismo ácido neoproterozóico do Escudo Sul-Rio-Grandense. Pesquisas Geoc. 30, 3-26.

680 Sommer, C.A., Lima, E.F., Nardi, L.V.S., Figueiredo, A.M.G., Pierosan, R., 2005. Potassic
681 and Low- and High-Ti Mildly Alkaline Volcanism in the Neoproterozoic Ramada Plateau,
682 Southernmost Brazil. J.S. Am. Earth Sci. 18, 237-254.

683 Sommer, C.A., Lima, E.F., Nardi, L.V.S, Liz, J. D., Waichel, B.L., 2006. The evolution of
684 Neoproterozoic magmatism in southernmost Brazil: shoshonitic, high-K tholeiitic and silica-
685 saturated, sodic alkaline volcanism in post-collisional basins. An. Acad. Bras. de Cienc. 78
686 (3), 573-589.

687 Streck, M.J., Grunder, A.L., 1995. Crystallization and welding variations in a widespread
688 ignimbrite sheet; the Rattlesnake Tuff, eastern Oregon, USA. Bull. Volcanol. 57, 151–169.

689 Streck, M.J., Grunder, A.L., 1997. Compositional gradients and gaps in the high-silica
690 rhyolites of the Rattlesnake Tuff, southeastern Oregon. J. Petrol. 38, 133– 163.

691 Walker, G.P.L., 1983. Ignimbrite types and ignimbrite problems. J. Volcanol. Geotherm. Res.
692 17, 65-88.

693 Watson, E.B., 1979. Zircon saturation in felsic liquids: experimental data and application to
694 trace element geochemistry. Contrib. Mineral. Petr. 70, 407-419.

695 Watson, E.B., Harrison, T.M., 1983. Zircon saturation revisited: temperature and composition
696 effects in a variety of crustal magma types. Earth Planet. Sc. Lett. 64, 295-304.

697 Whalen J.B., Currie K.L. Chappell B.W., 1987. A-type granites: geochemical characteristics,
698 discrimination and petrogenesis. Contrib. Mineral. Petrol. 95, 407-419.

699 Wildner, W., Nardi, L.V.S., Lima, E.F., 1999. Post-collisional Alkaline Magmatism on the
700 Taquarembó Plateau: a well Preserved Neoproterozoic-Cambrian Plutono-volcanic
701 Association in Southern Brazil. Int. Geol. Rev. 41, 1082-1098.

Wildner, W., Lima, E.F., Nardi, L.V.S., Sommer, C.A., 2002. Volcanic cycles and setting in the Neoproterozoic III to Ordovician Camaquã Basin succession in southern Brazil: characteristics of post-collisional magmatism. J. Volcanol. Geoth. Res. 118, 261-283.

Winchester, J.A., Floyd, P.A., 1977. Geochemical discrimination of different magma series and their differentiation products using immobile elements. Chem. Geol. 20, 325-343.

Wolff, J.A., Wright, J.V., 1981. Rheomorphism of welded tuffs. J. Volcanol. Geoth. Res. 10, 13-34.

FIGURE CAPTIONS

Figure 1 – Geological map of the western portion of the Sul-Rio-Grandense Shield, which shows the location of the Ramada and Taquarembó plateaus.

Figure 2 - Schematic stratigraphic profiles of the (a) Taquarembó and (b) Ramada Plateaus. The description of the facies codes (rheom LT, sLT(nl-ip), LT(nl), eLT, mLT, //bpL, crLT, sLl) are displayed in the table 1.

Figure 3 – Representative lithochemistry data of silicic volcanic rocks of the Acampamento Velho Formation: (a) SiO_2 x Zr/TiO_2 classification diagram (Winchester and Floyd, 1977); (b) R1-R2 classification diagram (De la Roche et al., 1980); (c) spidergram of trace elements normalised by ORG (Pearce et al., 1984); (d) REE diagram normalised by chondrite (Nakamura, 1974); (e) geotectonic diagram (Pearce et al. 1984); and (f) geotectonic diagram (Whalen et al., 1987). Legend: field in gray colour; representative composition of silicic volcanic rocks of the Acampamento Velho Formation.

Figure 4 –Schematic stratigraphic profile of the ignimbritic deposits of the Taquarembó Plateau. The description of the facies codes (rheom LT, sLT(nl-ip), LT(nl), eLT, mLT, //bpL,

727 crLT, sLl) are displayed in the table 1.

728 **Figure 5 –** Representative photomicrographies of ignimbrites in the Taquarembó Plateau that
729 illustrate the different degrees of welding: (a-c) = shards and pumice fragments in the welded
730 ignimbrite matrix related to stratified deposits; (d) fiamme in welded ignimbrite; (e) crystal
731 fragments, axiolites and eutaxitic texture in welded ignimbrite; (f) crystal and lithic fragments
732 in welded ignimbrite with eutaxitic texture; (g-h) parataxitic texture and rotated crystal
733 fragment related to rheomorphic ignimbrites.

734 **Figure 6 –** Schematic stratigraphic profile of ignimbrite deposits in the Ramada Plateau. The
735 description of the facies codes (rheom LT, sLT(nl-ip), LT(nl), eLT, mLT, //bpL, crLT, sLl)
736 are displayed in the table 1.

737 **Figure 7 –** Representative photomicrographs of ignimbrites on the Ramada Plateau showing
738 different degrees of welding: (a) welded ignimbrite rich in rhyolite fragments; (b) crystal-rich
739 welded ignimbrite; (c) shards and pumice fragments in welded ignimbrite; (d) crystal
740 fragments and pumice in welded ignimbrite with eutaxitic texture; (e) crystal fragments,
741 pumice and flattened shards in welded ignimbrite; (f) crystal fragments with stretched pumice
742 in rheomorphic ignimbrite; (g-h) crystal fragments and pumices in rheomorphic ignimbrite
743 with parataxitic texture.

744 **Figure 8 –** Diagrams displaying the relation of calculated temperature values with Zr (ppm)
745 content: (a) Ramada Plateau; (b) Taquarembó Plateau. Viscosity values in relation to
746 temperature for rheoignimbrites and ignimbrites of the Taquarembó and Ramada plateaus (c).
747 Legend: Ram rheo upper = rheoignimbrites of the upper portion of the Ramada Plateau; Ram
748 weld int = welded ignimbrites of the intermediate portion of the Ramada Plateau; Ram weld
749 low = welded ignimbrites of the lower portion of the Ramada Plateau; Taq rheo upper =
750 rheoignimbrites of the upper portion of the Taquarembó Plateau; Taq weld int = welded
751 ignimbrites of the intermediate portion of the Taquarembó Plateau; Taq weld low = welded
752 ignimbrites of the lower portion of the Taquarembó Plateau.

753

754 **Table 1 -** Terminology adopted to the characterization of the ignimbrite lithofacies of the
755 Acampamento Velho volcanism (modified from Branney and Kokelaar, 2002).

756 **Table 2 –** Lithochemistry data (major in % wt; trace in ppm), and temperature and viscosity
757 results of representative samples of the rheoignimbrites (rheom) and ignimbrites (ign) from
758 the Acampamento Velho Formation. Legend: samples CC = Taquarembó Plateau; samples
759 RM = Ramada Plateau.

Facies Cod.	Lithofacies Description
rheom LT	Massive, poorly sorted, vitriclastic matrix; strong flattening, rotational structures and high stretching
sLT(nl-ip)	Stratified lapilli-tuff, poorly sorted, normal grading of lithic fragments and reverse grading of pumice fragments
LT(nl)	Massive poorly sorted ignimbrite; normal graded lapilli-sized lithic fragments in ash-sized matrix
eLT	Lapilli-tuff with eutaxitic texture
mLT	Massive lapilli-tuff
//bpL	Welded rhyolitic ignimbrite with vitroclastic matrix; pumices lapilli flattened and aligned, defining a planar foliation subparallel to bedding
crLT	Crystal rich lapilli-tuff
sLl	Stratified lapilli-tuff, rich in lithic fragments

	CC02 Rheom	**CC08A** Rheom	**CC12A** Rheom	**CC25** Ign	**CC188** Ign	**CC74** Ign	**RM23A** Rheom	**RM22** Rheom	**RM86A** Rheom	**RM52** Ign	**RM111** Ign	**RM36** Ign
Localization/Plateau	Taquarembó						Ramada					
Flow unit	upper	upper	upper	intermediate	intermediate	lower	upper	upper	intermediate	intermediate	intermediate	lower
SiO_2	74.09	76.25	77.59	75.42	72.61	72.55	72.54	72.89	73.27	75.55	73.46	71.50
TiO_2	0.3	0.23	0.22	0.31	0.41	0.20	0.23	0.20	0.13	0.15	0.11	0.11
Al_2O_3	11.31	10.88	10.31	11.01	12.72	12.84	11.86	12.72	12.10	11.44	11.65	13.39
FeO_t	3.47	3.72	3.66	3.60	3.91	3.18	2.83	2.35	1.95	1.13	1.84	1.40
MnO	0.03	0.02	0.01	0.10	0.04	0.07	0.05	0.02	0.02	0.02	0.04	0.02
MgO	0.44	0.49	0.46	0.10	0.10	0.07	0.24	0.10	0.08	0.07	0.07	0.14
CaO	0.11	0.09	0.13	0.15	0.27	0.51	0.76	0.06	0.02	0.05	0.29	0.58
Na_2O	4.72	3.03	3.47	3.71	4.31	4.31	3.72	3.60	3.65	3.53	4.35	4.66
K_2O	4.26	4.25	3.96	4.17	3.90	4.19	5.11	5.53	5.73	5.06	4.95	4.68
P_2O_5	0.1	0.02	0.01	0.01	0.00	0.01	0.04	0.04	0.01	0.04	0.02	0.03
LOI	0.21	0.75	0.37	0.87	0.4	1.14	1.90	1.30	1.00	1.00	1.00	1.10
Total	99.29	100.02	100.45	99.79	99.01	99.23	99.6	99.07	98.16	98.17	97.98	97.77
IAGP	1.09	0.88	0.97	0.96	0.89	0.91	0.98	0.93	1.01	0.98	1.07	0.95
Ba	73	119	157	122	548	477	272	288	133	181	162	143
Rb	160	118	146	136	86	124	99	113	141	138	151	250
Sr	30	34	40	30	23	48	25	20	10	22	10	20
Zr	719	801	781	684	544	360	682	634	511	570	637	385
T Sat Zr (M) (^oC)	936	978	963	947	923	870	920	943	913	928	920	870
T liquid (^oC)	935	931	939	929	920	931	952	922	886	884	879	904
Viscosity												
logη (Pa s)	8.107	7.768	8.29	8.453	8.661	8.648	7.015	7.5	8.154	8.3	7.831	8.547

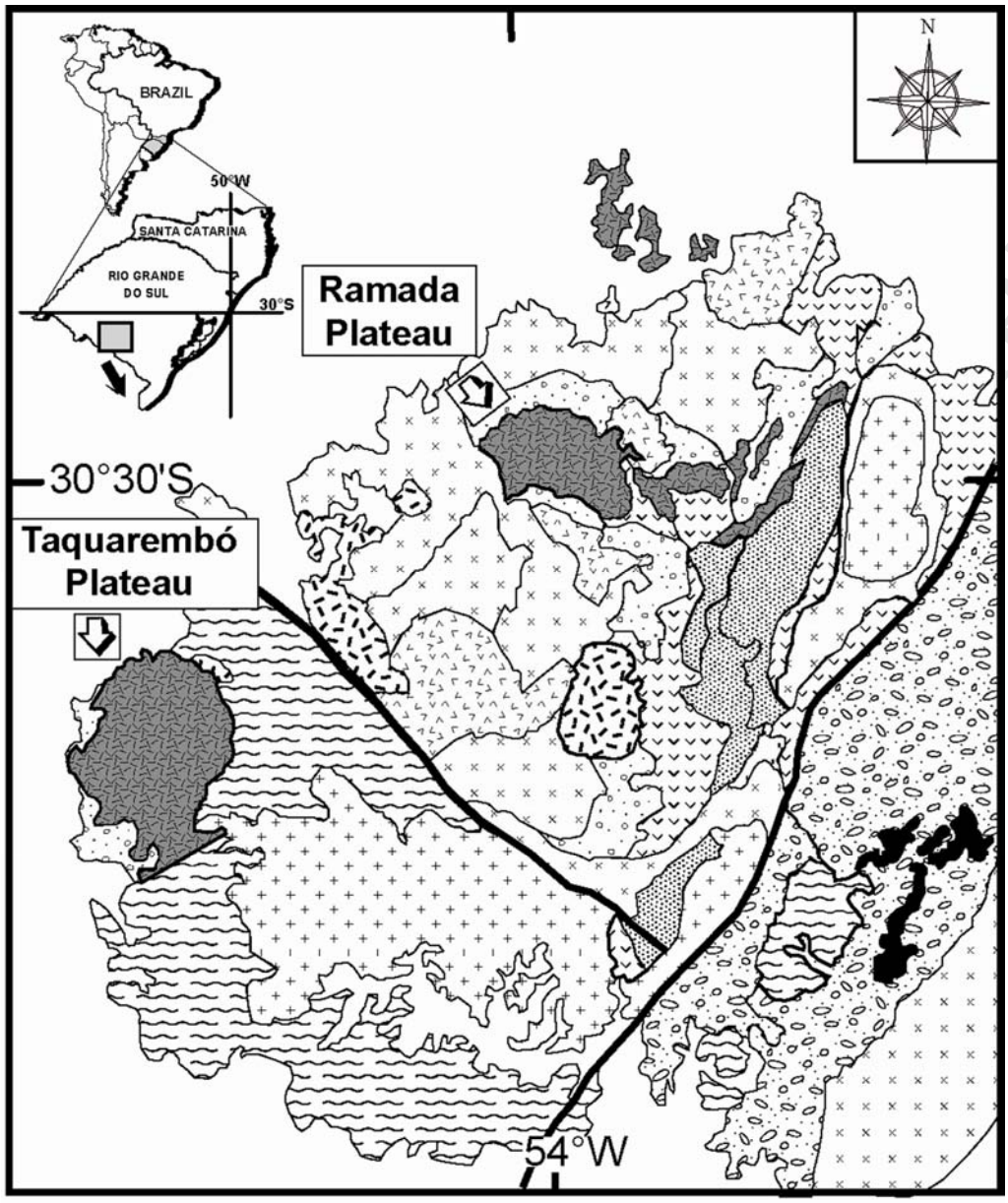
BRAZIL
50°W
SANTA CATARINA
RIO GRANDE DO SUL
30°S
N
Ramada Plateau
30°30'S
Taquarembó Plateau
54°W
0
20 km
CAMAQUÃ BASIN (650 - 470Ma)
Guaritas Group
Volcanic rocks (Rodeio Velho)
Sedimentary deposits
Santa Bárbara Group
(sedimentary deposits)
Cerro do Bugio Group
Acampamento Velho Formation
Bom Jardim Group
Hilario Formation
Maricá Group
(sedimentary deposits)
COEVAL GRANITIC MAGMATISM
(650-550 Ma)
Granitic rocks with alkaline affinity
Granitic rocks with shoshonitic affinity
Granitic rocks with high-K calc-alkaline affinity
Neoproterozoic Metamorphic Associations (800-700 Ma)
Santa Maria Chico Granulitic Complex (2.55 Ga)

(a) Taquarembó Plateau

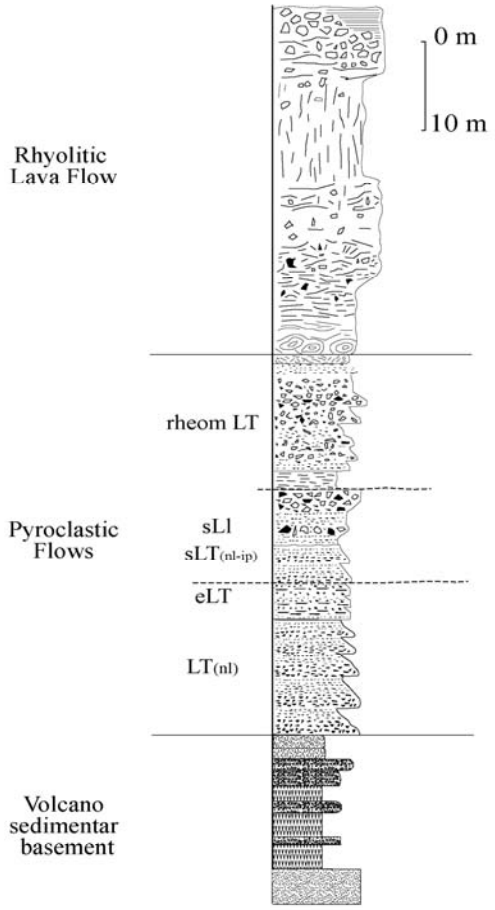

(b) Ramada Plateau

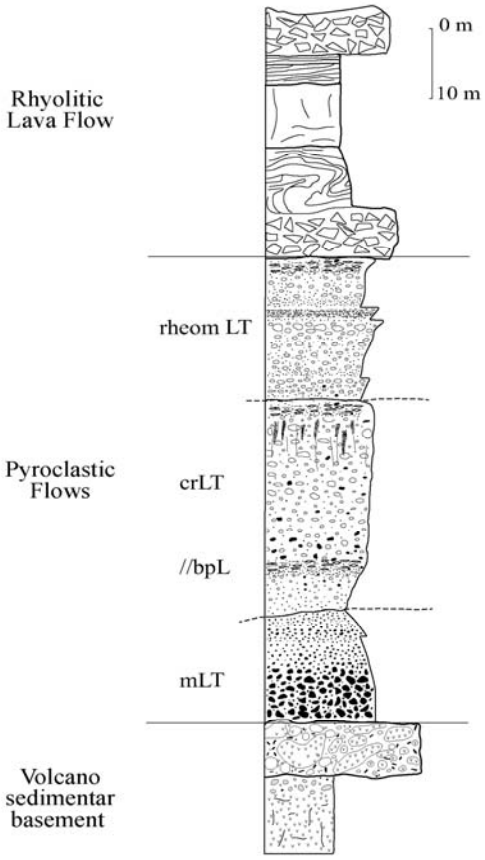

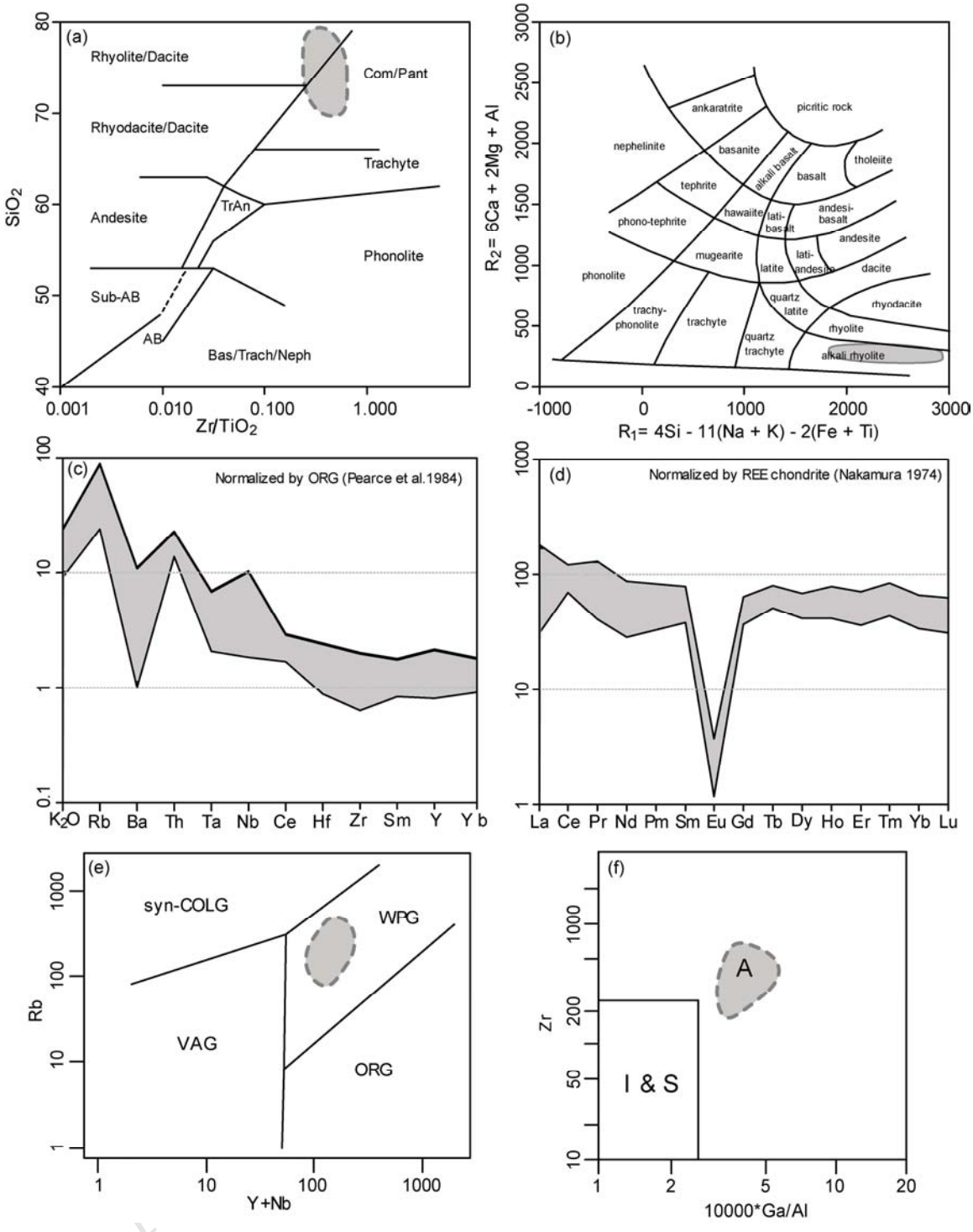
(a)
Rhyolite/Dacite
Com/Pant
Rhyodacite/Dacite
Trachyte
TrAn
Andesite
Phonolite
Sub-AB
AB
Bas/Trach/Neph
SiO2
Zr/TiO2
(b)
ankaratrite
picritic rock
nephelinite
basanite
alkali basalt
tholeiite
basalt
tephrite
hawaiite
lati-basalt
andesi-basalt
phono-tephrite
andesite
mugearite
lati-andesite
dacite
phonolite
latite
quartz latite
rhyodacite
trachy-phonolite
trachyte
rhyolite
quartz trachyte
alkali rhyolite
R2= 6Ca + 2Mg + Al
R1= 4Si - 11(Na + K) - 2(Fe + Ti)
(c)
Normalized by ORG (Pearce et al.1984)
K2O Rb Ba Th Ta Nb Ce Hf Zr Sm Y Yb
(d)
Normalized by REE chondrite (Nakamura 1974)
La Ce Pr Nd Pm Sm Eu Gd Tb Dy Ho Er Tm Yb Lu
(e)
syn-COLG
WPG
VAG
ORG
Rb
Y+Nb
(f)
A
I & S
Zr
10000*Ga/Al

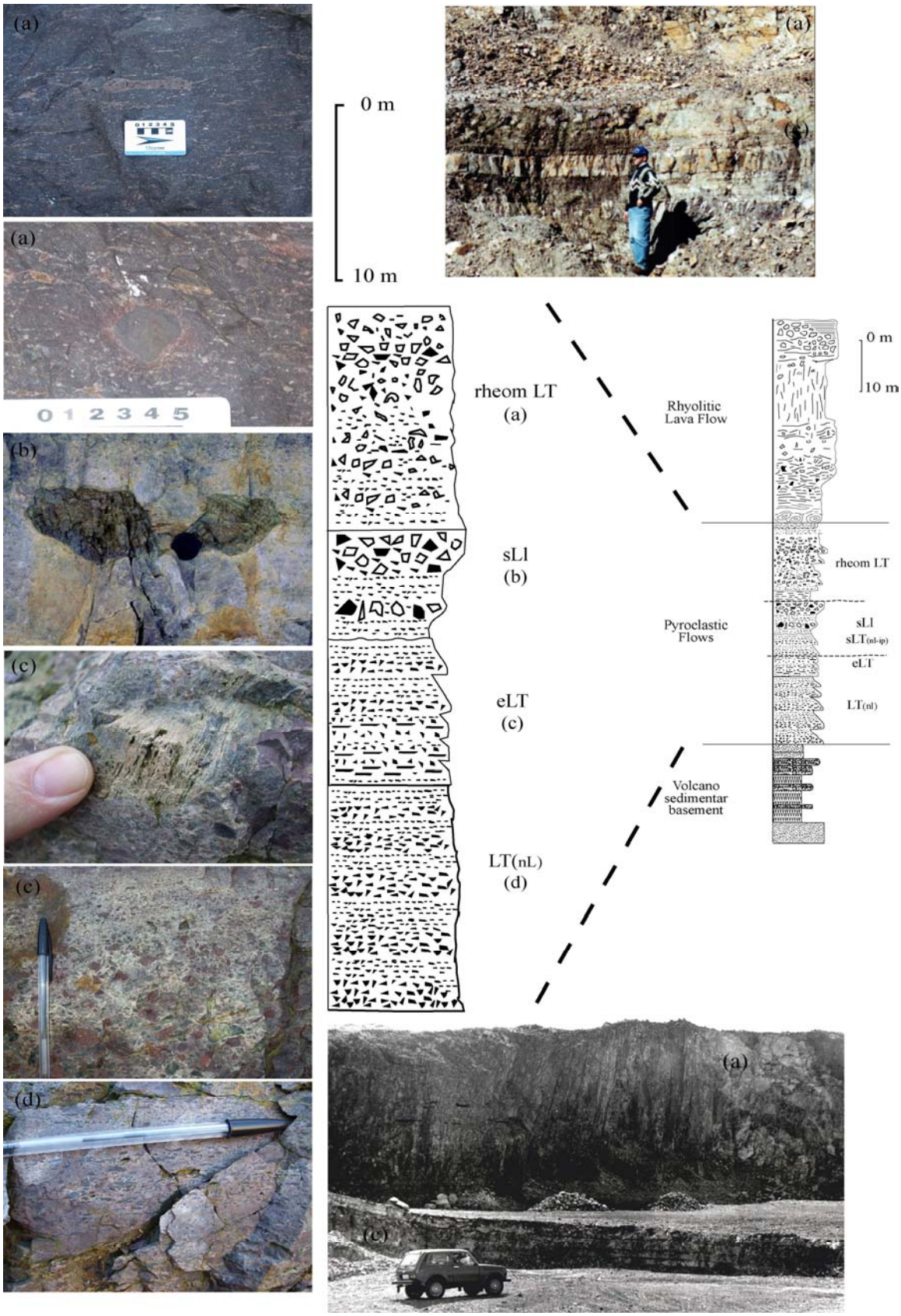
(a)
(a)
0 1 2 3 4 5
(b)
(c)
(c)
(d)
0 m
10 m
(a)
(b)
rheom LT
(a)
sLl
(b)
eLT
(c)
LT(nL)
(d)
Rhyolitic
Lava Flow
Pyroclastic
Flows
Volcano
sedimentar
basement
0 m
10 m
rheom LT
sLl
sLT(nl-ip)
eLT
LT(nl)
(a)
(c)

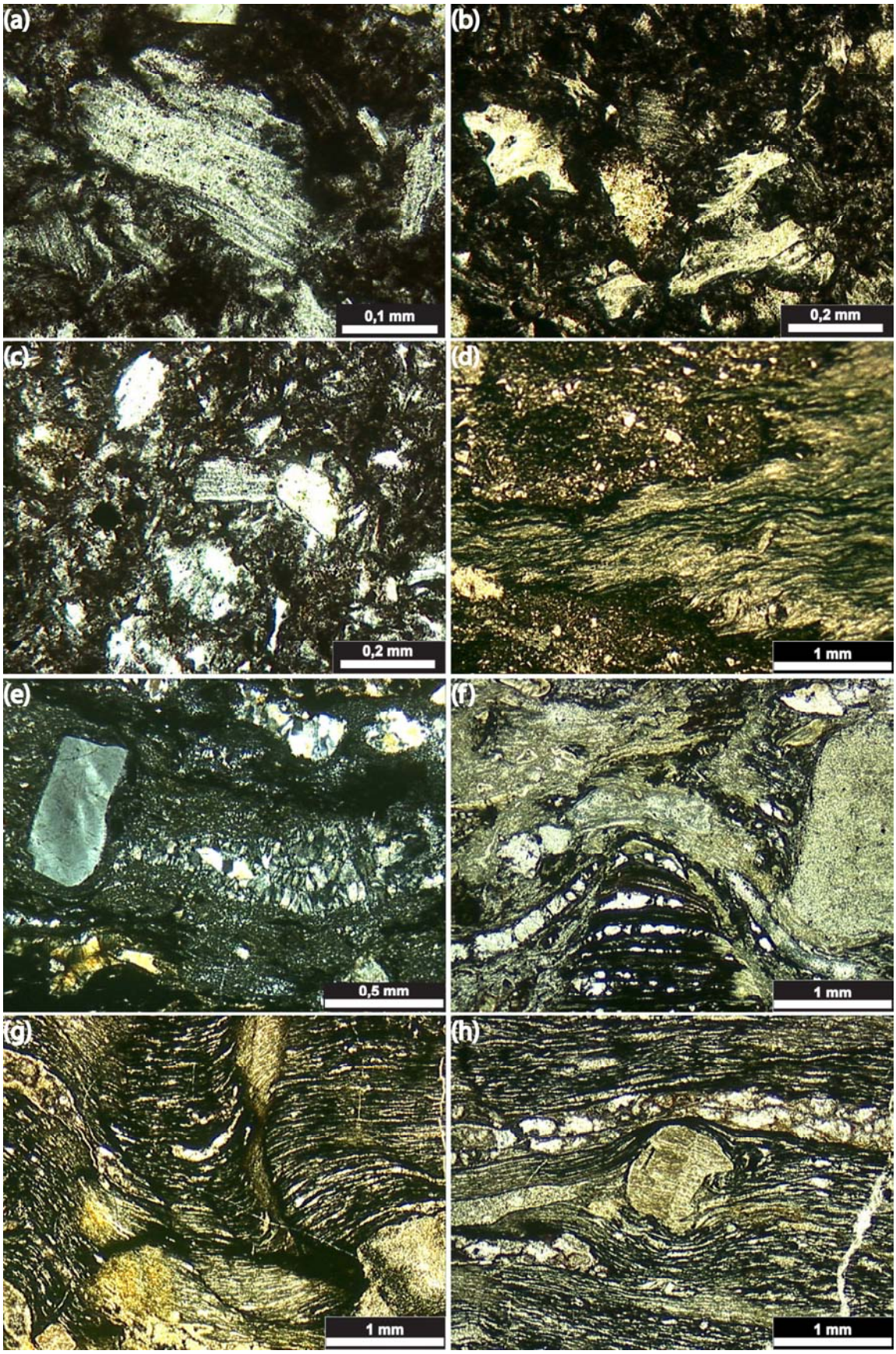
(a)
0,1 mm
(b)
0,2 mm
(c)
0,2 mm
(d)
1 mm
(e)
0,5 mm
(f)
1 mm
(g)
1 mm
(h)
1 mm

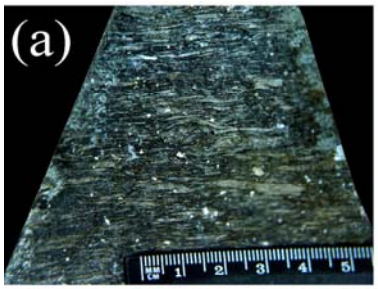
(a)

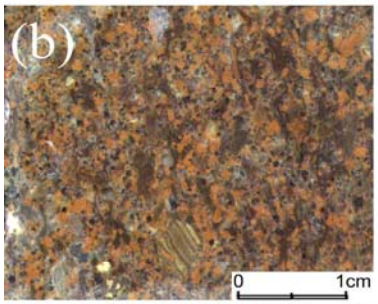
(b)
0
1cm


(c)

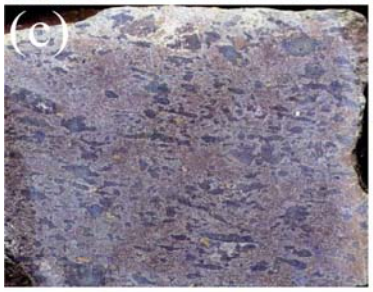
(c)


(d)


(d)

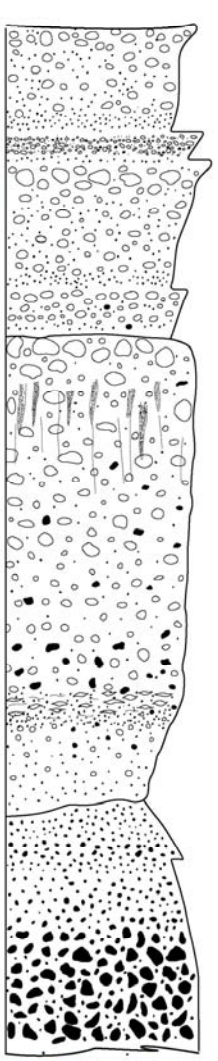
0 m
10 m
Rheom LT
(a)
CrLT
(b)
//bpL
(c)
mLT
(d)

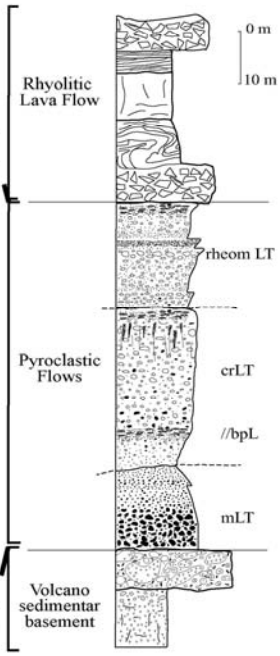
0 m
10 m
Rhyolitic
Lava Flow
rheom LT
Pyroclastic
Flows
crLT
//bpL
mLT
Volcano
sedimentar
basement

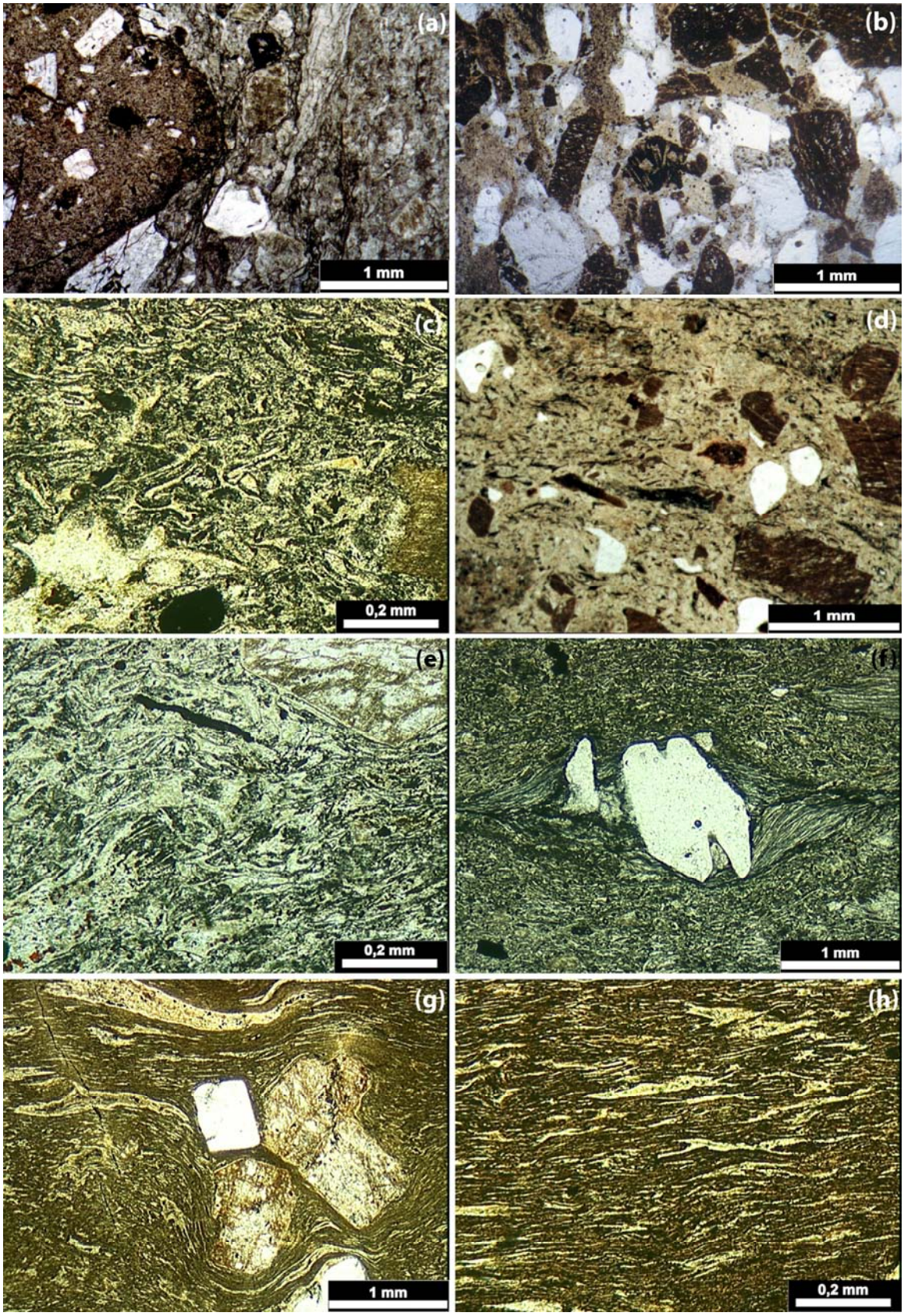
(a)
1 mm
(b)
1 mm
(c)
0,2 mm
(d)
1 mm
(e)
0,2 mm
(f)
1 mm
(g)
1 mm
(h)
0,2 mm

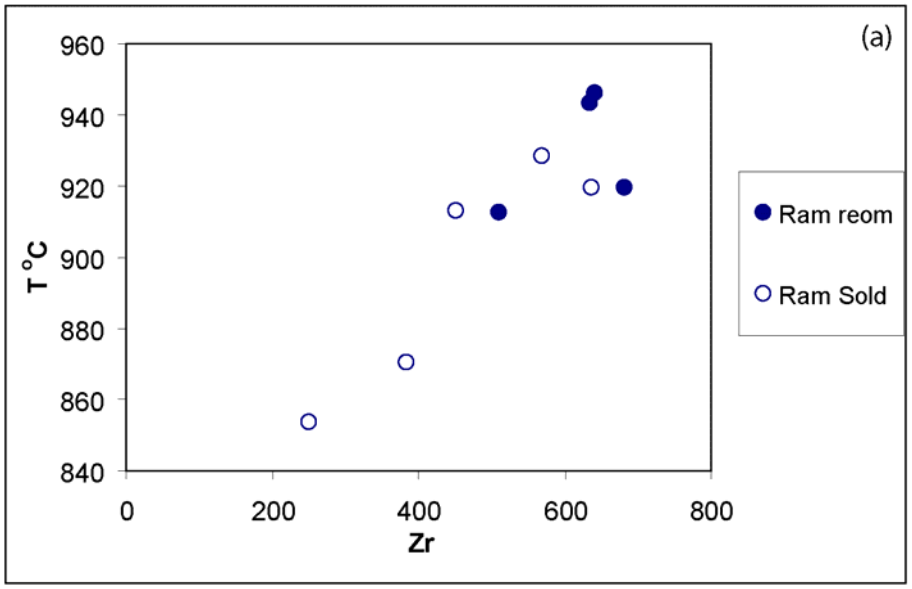
(a)
960
940
920
900
880
860
840
T °C
0
200
400
600
800
Zr
Ram reom
Ram Sold

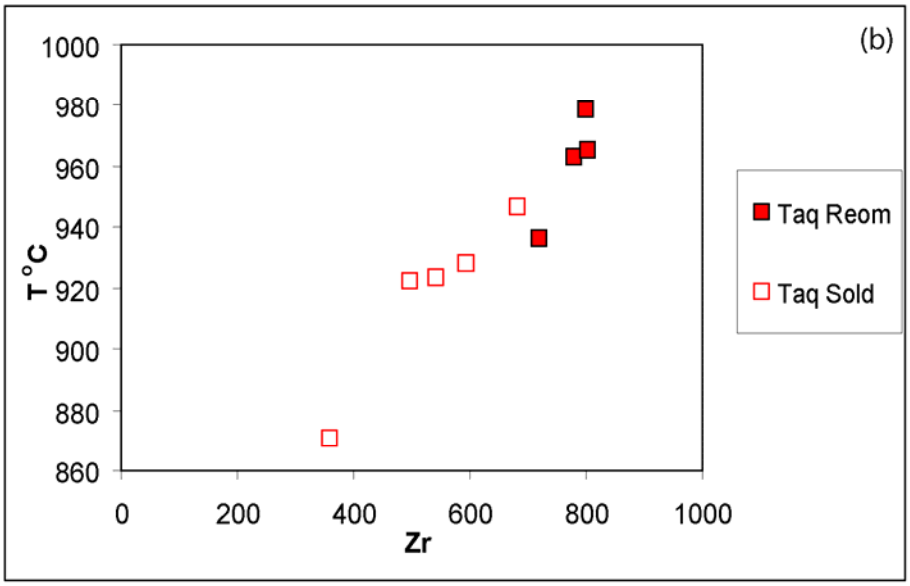
(b)
1000
980
960
940
920
900
880
860
T °C
0
200
400
600
800
1000
Zr
Taq Reom
Taq Sold

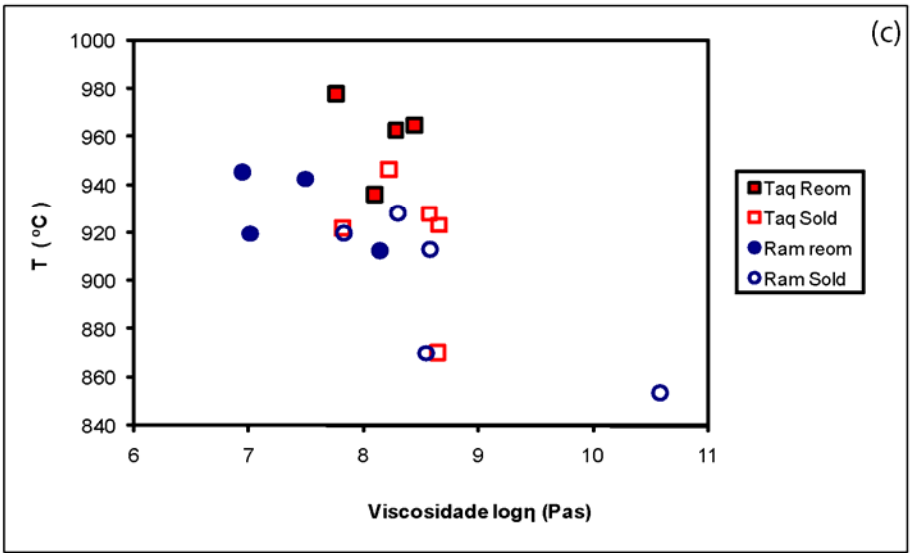
(c)
1000
980
960
940
920
900
880
860
840
T (°C)
6
7
8
9
10
11
Viscosidade logη (Pas)
Taq Reom
Taq Sold
Ram reom
Ram Sold